

# Development prospects and stability limits of mid-IR Kerr-lens mode-locked lasers

V.L. Kalashnikov, E. Sorokin, and I.T. Sorokina

Institut für Photonik, TU Wien, Gusshausstr. 27/387, A-1040 Vienna, Austria

## ABSTRACT

The Kerr-lens mode locking stability and the ultrashort pulse characteristics are analyzed numerically for the Cr-doped ZnTe, ZnSe, ZnS active media. The advantages of these materials for the femtosecond lasing within 2 - 3  $\mu\text{m}$  spectral range are demonstrated.

**Keywords:** ultrashort pulses, Kerr-lens mode-locking, mid-infrared solid-state lasers

## 1. INTRODUCTION

Compact diode-pumped sources of the femtosecond pulses tunable within the wavelength range between 2 and 3  $\mu\text{m}$  are of interest for various applications, such as laser surgery, remote sensing and monitoring, spectroscopy of semiconductors etc. To date only cryogenically operated Pb-salt diode lasers, optical parametrical oscillators and difference-frequency convertors were available for the operation in this spectral range. Therefore the possibility of the direct mid-IR lasing from the new class of the transition-metal doped chalcogenides<sup>1,2,3,4</sup> has attracted much attention. The impressive advantages of these media are room-temperature operation between 2 and 3  $\mu\text{m}$ , possibility of direct diode pumping, high emission and absorption cross-sections, negligibly low excited-state absorption and, as consequence, low thermal load (the basic laser material characteristics will be described in the next section). The most remarkable examples of the lasers under consideration are Cr<sup>2+</sup>-doped ZnSe, ZnS and ZnTe. To date the following achievements for these media have been demonstrated: 1) for Cr:ZnSe CW operation with over 1.7 W power,<sup>5</sup> over 1100 nm tunability,<sup>6</sup> over 350 nm tunable diode-pumped CW operation,<sup>7</sup> active mode locking<sup>8</sup> and active modulator assisted passive mode locking<sup>9</sup> were achieved; 2) for Cr:ZnS pulsed<sup>2,10</sup> and tunable CW operation<sup>11</sup> were obtained. Cr:ZnTe, which is a member of the considered media class, remains unexplored.

In spite of the numerous advantages, there exist some obstacles for femtosecond pulse generation from these lasers. As they are the semiconductors, i.e. possess a comparatively narrow band-gap, the nonlinear refraction in the active crystal is extremely large (see below). Hence the self-focusing has a low threshold which in the combination with the strong self-phase modulation produce a tendency to multiple pulse operation in the Kerr-lens mode locking (KLM) regime.<sup>9,12</sup> So there is a need in the study of KLM stability limits and methods of stability enhancement in the lasers under consideration.

In this paper we present the results of the numerical optimization of KLM aimed at the multipulsing suppression and taking into account a strong saturation of the Kerr-lens induced fast absorber. As a result, we demonstrate the possibility of few optical cycle generation from Cr-doped Zinc-chalcogenodes. The presented model is quite general and can be applied to the overall optimization of the different KLM lasers.

## 2. MODEL AND BASIC PARAMETERS

Simulation of the KLM can be based on the two quite different approaches. First one supposes the full-dimensional modelling taking into account the details of the field propagation in the laser cavity.<sup>13</sup> The minimal dimension of such models is 2+1 and the optimization procedure needs mainframe computing. Although this approach allows the description of the spatio-temporal dynamics of the ultrashort pulses and their mode pattern, its main disadvantages are the large number of the parameters resulting in ambiguity of the optimization procedure and complexity of the interpretation of the obtained results. Second approach is based on 1+1 dimensional model in the framework of the so-called nonlinear Ginzburg-Landau equation,<sup>14</sup> which describes the KLM as an action of the fast saturable absorber governed by few physically meaningful parameters, viz., its modulation depth  $\gamma$  and the inverse saturation

---

Further author information: (Send correspondence to Dr. V.L. Kalashnikov)

V.L. Kalashnikov: E-mail: v.kalashnikov@tuwien.ac.at

intensity  $\sigma$ . This method allows the analytical realization in the weak-nonlinear limit,<sup>15</sup> however in the general case the numerical simulations are necessary. We shall be based on the latter approach in view of its physical unambiguity.

The master equation describing the ultrashort pulse generation in the KLM solid-state laser is:

$$\frac{\partial a(z,t)}{\partial z} = \left[ \alpha - \rho + \left( t_f^2 - i \sum_{m=2}^N \frac{(-i)^m \beta_m}{m!} \frac{\partial^m}{\partial t^m} \right) - \frac{\gamma}{1 + \sigma |a(z,t)|^2} - i\delta \left( |a(z,t)|^2 - \frac{i}{\omega_0} \frac{\partial}{\partial t} |a(z,t)|^2 \right) \right] a(z,t), \quad (1)$$

where  $a(z,t)$  is the field amplitude (so that  $|a|^2$  has a dimension of the intensity),  $z$  is the longitudinal coordinate normalized to the cavity length (thus, as a matter of fact, this is the cavity round-trip number),  $t$  is the local time,  $\alpha$  is the saturated gain coefficient,  $\rho$  is the linear net-loss coefficient taking into account the intracavity and output losses,  $t_f$  is the group delay caused by the spectral filtering within the cavity,  $\beta_m$  is the  $m$ -order group-delay dispersion (GDD) coefficients,  $\delta = l_g n_2 \omega_0 / c = 2\pi n_2 l_g / (\lambda_0 n)$  is the self-phase modulation (SPM) coefficient,  $\omega_0$  and  $\lambda_0$  are the frequency and wavelength corresponding to the minimum spectral loss,  $n$  and  $n_2$  are the linear and nonlinear refraction coefficients, respectively,  $l_g$  is the double length of the gain medium (we suppose that the gain medium gives a main contribution to the SPM). The last term in Eq. (1) describes the self-steepening effect and for the simplification will be not taken into account in the simulations. As an additional simplification we neglect the stimulated Raman scattering in the active medium.<sup>16</sup> These two factors will be considered hereafter.

The gain coefficient obeys the following equation:

$$\frac{\partial \alpha(z,t)}{\partial t} = \sigma_a (\alpha_{\max} - \alpha(z,t)) \frac{I_p}{\hbar \omega_p} - \sigma_g \alpha(z,t) \frac{|a(z,t)|^2}{\hbar \omega_0} - \frac{\alpha(z,t)}{T_r}. \quad (2)$$

Here  $\sigma_a$  and  $\sigma_g$  are the absorption and emission cross-sections of the active medium, respectively,  $T_r$  is the gain relaxation time,  $I_p$  is the absorbed pump intensity,  $\omega_p$  is the pump frequency,  $\alpha_{\max} = \sigma_g N_g l_g$  is the maximum gain coefficient,  $N_g$  is the concentration of the active centers. The assumption  $\tau_p \ll T_{cav}$  ( $\tau_p$  is the pulse duration,  $T_{cav}$  is the cavity period) allows the integration of Eq. (2). Then for the steady-state gain coefficient we have:

$$\alpha = \frac{\alpha_{\max} \sigma_a I_p T_{cav}}{\hbar \omega_p \left( \frac{\sigma_a I_p T_{cav}}{\hbar \omega_p} + \frac{E}{E_s} + \frac{T_{cav}}{T_r} \right)}, \quad (3)$$

where  $E_s = \hbar \omega_p / \sigma_g$  is the gain saturation energy flux,  $E = \int_{-T_{cav}/2}^{T_{cav}/2} |a(t)|^2 dt$  is the pulse energy.

For the numerical simulations it is convenient to normalize the time and the intensity to  $t_f = \lambda_0^2 / (\Delta \lambda c)$  and  $1/\delta$ , respectively ( $\Delta \lambda$  is the gain bandwidth). The simulation were performed on the  $2^{12} \times 10^4$  mesh. Only steady-state pulses were considered. As the criterion of the steady-state operation we chose the peak intensity change less than 1% over last 1000 cavity transits.

The KLM in the considered model is governed by only four basic parameters:  $\alpha - \rho$ ,  $\beta_2$ ,  $\gamma$ , and  $\sigma$ . This allows unambiguous multiparametric optimization. In the presence of the higher-order GDD, the additional  $\beta_m$  parameters appear. This complicates the optimization procedure, but keeps its physical clarity.

Now let us to give the basic material parameters governing the femtosecond oscillation in the lasers under consideration.

**Table 1.** Material parameters of the Cr-doped Zinc-chalcogenides.

Medium	$\lambda_0$ , $\mu\text{m}$	$\Delta\lambda$ , nm	$\lambda_a$ , $\mu\text{m}$	$\sigma_a$ , $10^{-19}$ cm <sup>2</sup>	$\sigma_g$ , $10^{-19}$ cm <sup>2</sup>	$n$	$n_2$ , $10^{-13}$ esu	$T_r$ , $\mu\text{s}$
Cr:ZnSe	2.5	880	1.61	8.7	9	2.44	170	6-8
Cr:ZnS	2.35	800	1.61	5.2	7.5	2.3	48	4-11
Cr:ZnTe	2.6	800	1.61	12	20	2.71	830	3

It should be noted that the  $n$  values correspond to  $\lambda_0$ , but the experimentally observed  $n_2$  correspond to  $\lambda=1.06 \mu\text{m}$  (see Ref.<sup>17</sup>). As a result, we need the theoretical estimation of their values at the generation wavelength. Such estimation can be obtained from the formula <sup>17</sup>:

$$n_2(esu) = K \frac{G(\hbar\omega/E_g)\sqrt{E_p}}{nE_g^4},$$

where  $K = (0.5 - 1.5)\times 10^{-8}$  and  $E_p = 21 \text{ eV}$  are the material independent constants,  $E_g$  is the band-gap width in eV,  $G$  is the form-factor. Using for  $K$  the value, which produces the best agreement with the experimental values of  $n_2$ , we can obtain the following estimations:

**Table 2.** Estimations of  $n_2$  at  $\lambda_0$ .

	ZnSe	ZnS	ZnTe
$n_2, 10^{-13} \text{ esu}$	82	25	380

We note that the semiconductor nature of the considered active media results in the extremely high nonlinear refraction coefficients in the comparison with Ti:sapphire, for example ( $1.2\times 10^{-13} \text{ esu}$ ). As it will be shown below, this has a pronounced manifestation in the femtosecond pulse dynamics.

The simulation parameters corresponding to the above introduced normalizations are summarized in Table 3 ( $P = \sigma_{14}T_{cav}I_p/(\hbar\omega_0)$ ,  $\epsilon = t_f E_s^{-1}/\delta$ ).

**Table 3.** Simulation parameters.  $l_g=2\times 0.3 \text{ cm}$ ,  $T_{cav}=10 \text{ ns}$ ,  $2 \text{ W}$  pump power,  $100\times 100 \mu\text{m}^2$  pump mode.

Medium	$\alpha_{max}$	$n_2, 10^{-16} \text{ cm}^2/\text{W}$	$\delta, 10^{-12} \text{ cm}^2/\text{W}$	$\epsilon, 10^{-4}$	$t_f, \text{ fs}$	$P, 10^{-3}$
Cr:ZnSe	5	141	87	4.9	3.8	1.1
Cr:ZnS	5	45.5	32	10	3.7	0.62
Cr:ZnTe	5	587	314	3.8	4.5	1.9

### 3. RESULTS AND DISCUSSION

First of all we have to consider the meaning of the optimization procedure. The numerical simulations demonstrate that there exist some values of the saturation parameter  $\sigma$ , which provide the near chirp-free pulse generation. These values of  $\sigma$  can be considered as “optimal”. However, there is the additional factor, which has to be taken into account: the pulse shortening is possible by the  $\sigma$  growth and  $\beta_2 \rightarrow 0$ . We consider the values of  $\beta_2$  and  $\sigma$  as optimal if they correspond to the generation of the shortest pulse. The main obstacle on the way of the pulse shortening is the multiple pulse generation.<sup>12</sup> The strong tendency to the multipulsing results from 1)  $E_s^{-1}$  decrease, 2)  $P$  increase, 3) fast absorber saturation favored by the large  $\sigma$ . The relatively large values of  $\sigma_g$  and  $\lambda_0$  for the considered media result in the increase of the first parameter. However, the large absorption cross sections and SPM coefficients increase two later parameters. If the growth of the first parameter corresponds to the gain saturation and thereby to the stabilization of the pulse against the laser continuum growth, the larger  $P$  and  $\sigma$  initiate the rise of the continuum and the excitation of the perturbations inside the ultrashort pulse.<sup>18</sup> Hence, the optimization means the multiple pulses suppression allowing the pulse shortening.

Additional limitations on the pulse shortening result from the achievable values of the saturation parameter  $\sigma$ . In the KLM lasers this parameters is governed by the cavity alignment: the shift towards the cavity stability zone increases  $\sigma$ . So, the highest values of  $\sigma$  are reached in the immediate vicinity of the cavity stability boundary. This demands a too thorough cavity optimization and can not be considered as operational. Hence, the optimization aimed at the pulse shortening is based on the variation of all four parameters of the master Eq. (1) and is constrained by the above described reasons.

Fig. 1 shows the parameters of Eq. (1), which for the fixed  $\alpha - \rho$ ,  $\gamma$  and  $\sigma$  correspond to the minimum achievable  $\beta_2$  where the pulse has a minimum. The further  $\beta_2$  decrease results in the multipulse operation. Thus, the points in

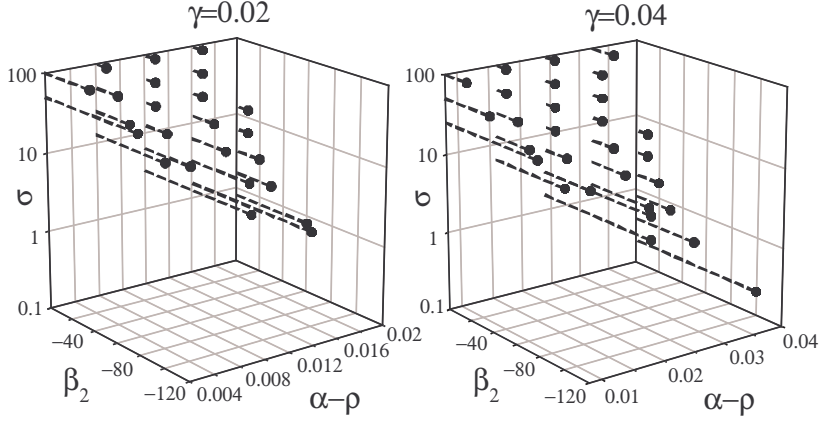


**Figure 1.** Stability boundary for the single pulse operation.

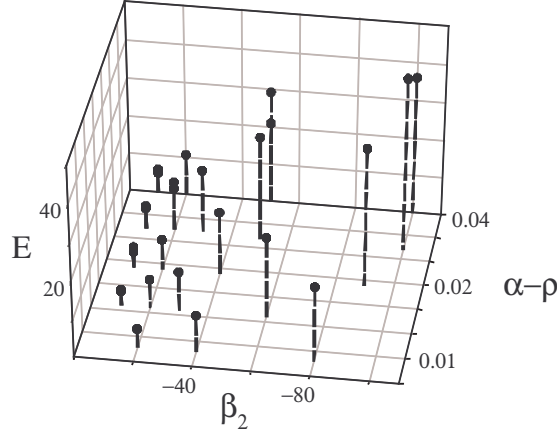


**Figure 2.** Pulse energy  $E$  on the stability boundary for  $\gamma=0.04$ .

Fig. 1 lie on the boundary of the stable single pulse operation. There is a set of the general tendencies characterizing this boundary.

There exists a limited on  $\alpha - \rho$  range of the stable single pulse operation, which expands as a result of the  $\sigma$  and  $\gamma$  growth. The increase of  $\sigma$  shifts this region towards the smaller  $\alpha - \rho$ . However, when  $\sigma > 100$  the transition to multipulsing is possible. As every point in Fig. 1 corresponds to the fixed dimensionless  $E$  (see Fig. 2), the choice of the appropriate level of  $\alpha - \rho$  for the fixed laser configuration (i.e. fixed  $\gamma$ ,  $\sigma$  and  $\beta_2$ ) is realized by the variation of  $P$  (pump, see Eq. (3)) as well as  $\rho$  (output loss). It is possible also to change  $\alpha$  by the change of  $\alpha_{max}$  due to variation of the crystal length or the active ions concentration or by the change of  $T_r$  due to variation of the active ions concentration. Note also, that the  $l_g$  decrease increases  $\epsilon$  (due to the  $\delta$  decrease), which describes the “strength” of the gain saturation relatively the SPM, and thereby increases  $P$  providing some fixed  $\alpha$ . Hence,  $\epsilon$  increase expands the stability region towards the higher pump and allows the higher pulse energies (because they  $\propto 1/\delta$ ).

The  $E$  decrease for the fixed  $\alpha - \rho$ , which takes a place for  $\beta_2 \rightarrow 0$  (Fig. 2), has to be accompanied by  $P$ ,  $\alpha_{max}$ ,  $T_r$  decrease or by  $\epsilon$ ,  $\rho$  increase in order to prevent from the continuum amplification. The last is the main source of the pulse destabilization and suppresses the single pulse operation in the vicinity of zero GDD. Hence, the pulse generation for  $\alpha - \rho - \gamma > 0$  is not possible.  $\alpha - \rho - \gamma = 0$  corresponds to the specific hybrid regime with the coexistent

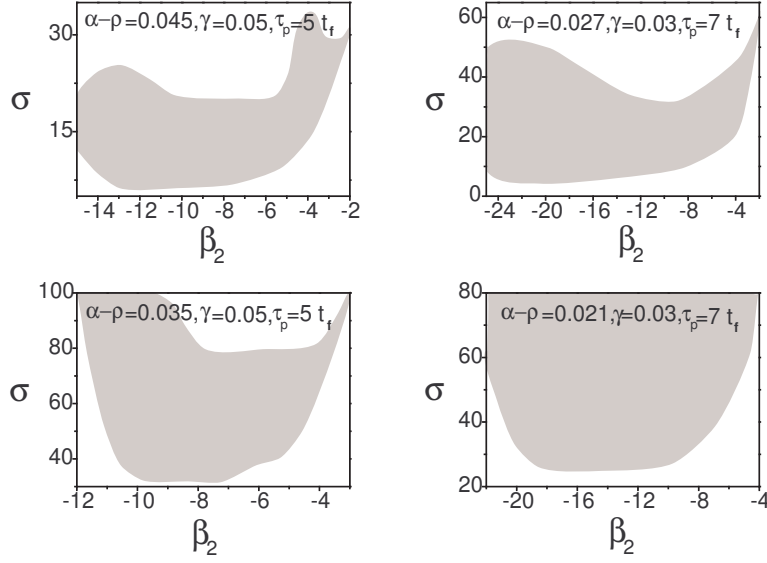


**Figure 3.** Regions of the  $\sigma$  and  $\beta_2$  parameters providing the shortest pulses.

pulse and continuum .<sup>19</sup>

Since the approach of GDD to zero has to be accompanied by the pump decrease, this results in the growth of the  $\sigma$  required for the pulse stabilization (Fig. 1). This can demand too thorough cavity alignment. Moreover, for the large  $\sigma$  we need the larger minimum  $|\beta_2|$  providing the single pulse operation so that the dependence of the minimum  $|\beta_2|$  on the  $\sigma$  for the fixed  $\alpha - \rho$  has a parabolic-like form .<sup>18</sup>

The most interesting features are the shift of the stability region towards the smaller  $\sigma$  (Fig. 1) and the pulse shortening as a result of the  $\gamma$  increase. For example, the minimum pulse duration  $\tau_p$  for  $\gamma = 0.03$  is  $7t_f$  whereas for  $\gamma = 0.05$  it is  $5t_f$  (this is 19 fs for Cr:ZnSe and Cr:ZnS and 23 fs for Cr:ZnTe). The bad news here is the need for the hard-aperture KLM to provide the larger modulation depth. This reduces the KLM self-starting ability.

The regions of the parameters allowing the shortest pulses are shown in Fig. 3. The  $\alpha - \rho$  increase reduces the minimum  $\sigma$  parameter producing the shortest pulses. However the region of their existence shortens on  $\sigma$ . The  $\tau_p$  growth enlarges the corresponding region.

Let us consider the concrete parameters of Table 3. The pump thresholds allowing  $7t_f$  pulse durations are shown in Fig. 4. The threshold decreases from Cr:ZnS through Cr:ZnSe to Cr:ZnTe that results from the  $\epsilon$  decrease. This means that the SPM becomes stronger relatively the gain saturation under this transition. As a result, the tendency to the pulse destabilization intensifies and this demands to reduce the intracavity power by means of the pump decrease.

Thus, the  $\epsilon$  decrease reducing KLM threshold turns in the intracavity pulse energy decrease (Fig. 5). The highest value of  $\epsilon$  for Cr:ZnS resulting from the large  $\sigma_g$  in the combination with comparatively small  $\delta$  produces the stabilization of the shortest pulses with the highest energies.

Note, that the larger absorption cross-section for Cr:ZnTe results in the highest absorbed pump energy for the fixed pump intensity and mode area. This is a positive factor for the KLM threshold lowering. However, this can be a negative factor, when the SPM is the source of the pulse destabilization because the additional efforts for the intracavity power decrease are necessary.

At last, we consider the contribution of the third-order dispersion, which can be large for the lasers under consideration. There are the technological troubles in the use of the chirped-mirror technique for the dispersion compensation in the mid-IR due to high value of  $\lambda_0$ . Therefore the usual technique utilizing the prisms for the dispersion control can be useful in the considered situation. As a result, the third-order net-dispersion coefficient  $|\beta_3|$  increases.

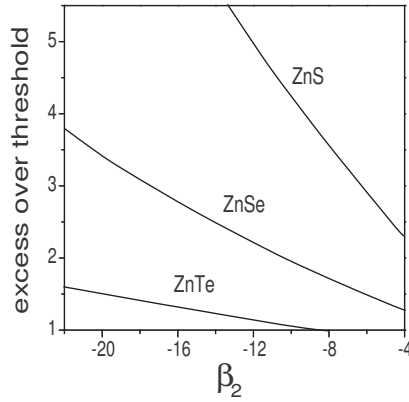


**Figure 4.** Pump threshold of KLM related to that for CW. Pulse duration is  $\tau_p = 7 t_f$ .  $\alpha = 0.071$ ,  $\rho = 0.05$ ,  $\gamma = 0.03$ ,  $\alpha_{max} = 5$ , other parameters correspond to Table 3.

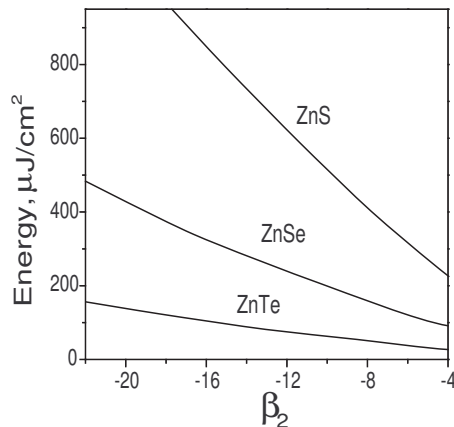


**Figure 5.** Intracavity pulse energy fluxes. The parameters correspond to Fig. 4.

For the simulation we choose  $\beta_3 = -5900 \text{ fs}^3$ . As it can be seen from Fig. 6, the shape of the stability boundary does not change in the comparison to  $\beta_3 = 0$ .<sup>20</sup> However, the minimum pulse duration increases from  $5t_f$  for  $\beta_3 = 0$  to  $9t_f$  (34 fs for Cr:ZnS, Cr:ZnSe and 40 fs for Cr:ZnTe). The additional effect is the pronounced (up to 140 nm) Stokes shift of the peak wavelength (Fig. 6 shows this shift on the stability boundary for Cr:ZnSe and Cr:ZnS). This shift is typical also for such IR lasers as Cr:LiSGaF, Cr:LiSAF, Cr<sup>4+</sup>:YAG<sup>16,20</sup> and can reduce the pulse energy due worse overlap between gain band and pulse spectrum. However, for the media under consideration the wavelength shift is small in comparison to the full gain band width and the energy decrease is not critical.

#### 4. CONCLUSION

In conclusion, we presented the model, which can be usable for the numerical optimization of the KLM lasers and is governed by only four basic parameters: difference between saturated gain and linear loss, GDD, modulation depth and saturation intensity of the fast saturable absorber. On the basis of this model, the KLM abilities of the Cr-doped Zinc-chalcogenides were estimated. It was shown, that the strong SPM inherent to these media and destabilizing the single pulse operation can be overcome by the choice of the appropriate GDD, pump, modulation depth and saturation parameter of the Kerr-lensing induced fast saturable absorber. It was demonstrated also, that the continuum amplification is reduced by the large gain saturation and the destabilizing nonlinear phase shift decreases due to high linear refraction and large generation wavelength in the media under consideration. As a result,

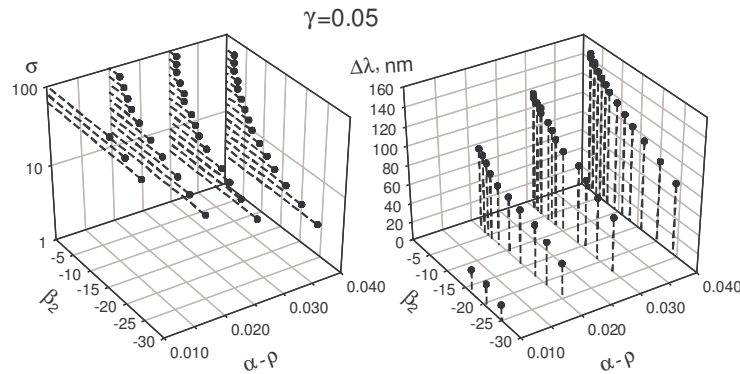


**Figure 6.** Stability boundary for the single pulse operation in the presence of the third-order dispersion and the Stokes spectral shift of the pulse spectrum on this boundary.

the Cr:ZnTe possesses the lowest KLM threshold, however strong SPM constrains the achievable pulse power for this laser. The best stability for the highest energy flux and the shortest pulse duration (19 fs) are achievable in Cr:ZnS. Cr:ZnSe lies between these media. The presence of the third-order dispersion increases the minimum achievable pulse durations up to 34 - 40 fs and causes the strong (up to 140 nm) Stokes shift of the generation wavelength. However, the latter effect does not reduce noticeably the pulse energy. On the whole, the Cr-doped Zinc-chalcogenides have the prospects of sub-50 fs generation that amounts to only few optical cycles around 2.5  $\mu\text{m}$ .

## ACKNOWLEDGMENTS

This work was supported by Austrian National Science Fund Project M688.

## REFERENCES

1. L.D. DeLoach, R.H. Page, G.D. Wilke, S.A. Payne, and W.F. Krupke. "Transition metal-doped Zinc chalcogenides: spectroscopy and laser demonstration of a new class of gain media," *IEEE J. Quantum Electron.* **32**, pp. 885–895, 1996.
2. R.H. Page, K.I. Schaffers, L.D. DeLoach, G.D. Wilke, F.D. Patel, J.B. Tassano, S.A. Payne, W.F. Krupke, K.-T. Chen, A. Burger. "Cr<sup>2+</sup>:doped Zinc chalcogenides as efficient widely tunable mid-infrared lasers," *IEEE J. Quantum Electron.* **33**, pp. 609–619, 1997.
3. U. Hömmerich, X. Wu, V.D. Davis, S.B. Trivedi, K. Grasze, R.J. Chen, S.W. Kutcher. "Demonstration of room-temperature laser action at 2.5  $\mu\text{m}$  from Cr<sup>2+</sup>:Cd<sub>0.85</sub>Mn<sub>0.15</sub>Te," *Optics Lett.* **22**, pp. 1180–1182, 1997.
4. J. McKay, K.L. Schepler, G.C. Catella. "Efficient grating-tuned mid-infrared Cr<sup>2+</sup>:CdSe laser," *Optics Lett.* **24**, pp. 1575–1577, 1999.
5. G.J. Wagner, T.J. Carrig. "Power scaling of Cr<sup>2+</sup>:ZnSe lasers," in *OSA Trends in Optics and Photonics*, vol. 50, *Advanced Solid-State Lasers*, Cr. Marshall, ed. (OSA, Washington DC 2001), pp. 506–510.
6. I.T. Sorokina, E. Sorokin, A. DiLieto, M. Tonelli, R.H. Page. "Tunable diode-pumped continuous-wave operation and passive mode-locking of Cr<sup>2+</sup>:ZnSe laser," in *Conference on Lasers and Electro-Optics/Europe 2001*, Conference Digest, München, p. 151, 2001.
7. E. Sorokin, I.T. Sorokina. "Tunable diode-pumped continuous-wave Cr<sup>2+</sup>:ZnSe laser," *Applied Physics Lett.*, **80**, pp. 3289–3291, 2002.
8. T.J. Carrig, G.J. Wagner, A. Sennaroglu, J.Y. Jeong, C.R. Pollock. "Mode-locked Cr<sup>2+</sup>:ZnSe laser", *Optics Lett.*, **25**, pp. 168–170, 2000.
9. E. Sorokin, I.T. Sorokina, R.H. Page. "Room-temperature CW diode-pumped Cr<sup>2+</sup>:ZnSe laser", in *OSA Trends in Optics and Photonics*, vol. 50, *Advanced Solid-State Lasers*, Cr. Marshall, ed. (OSA, Washington DC 2001), pp. 101–105.

10. K. Graham, S. Mirov, V. Fedorov, M.E. Zvanut, A. Avanesov, V. Badikov, B. Ignat'ev, V. Panutin, G. Shevirdayeva. "Spectroscopic characteristics and laser performance of diffusion doped  $\text{Cr}^{2+}:\text{ZnS}$ ," in *OSA Trends in Optics and Photonics*, vol. 50, *Advanced Solid-State Lasers*, Cr. Marshall, ed. (OSA, Washington DC 2001), pp. 561–567.
11. I.T. Sorokina, E. Sorokin, S. Mirov, V. Fedorov, V. Badikov, V. Panyutin, K.I. Schaffers. "Broadly tunable compact continuous-wave  $\text{Cr}^{2+}:\text{ZnS}$  laser," *Optics Lett.* , **27**, pp. 1040–1042, 2002.
12. V.L. Kalashnikov, E. Sorokin, I.T. Sorokina. "Multipulse operation and limits of the Kerr-lens mode locking stability for  $\text{Cr}^{2+}:\text{ZnSe}$  laser," in *OSA Trends in Optics and Photonics*, vol. 65, *Advanced Solid-State Lasers*, M.E. Fermann, L.R. Marshall, eds. (OSA, Washington DC 2002), pp. 374–378.
13. V.P. Kalosha, M. Müller, J. Herrmann, and S. Gatz. "Spatiotemporal model of femtosecond pulse generation in Kerr-lens mode-locked solid-state lasers", *J. Opt. Soc. Am. B*, **15**, pp. 535-550, 1998.
14. I.S. Aranson, L. Kramer. "The world of the complex Ginzburg-Landau equation", *Rev. Modern Physics*, **74**, pp. 99-143, 2002.
15. H.A. Haus, J.G. Fujimoto, E.P. Ippen. "Analytic theory of additive pulse and Kerr lens mode locking", *IEEE J. Quantum Electron.* **28**, pp. 2086–2096, 1992.
16. V.L. Kalashnikov, E. Sorokin, I.T. Sorokina. "Mechanisms of spectral shift in ultrashort-pulse laser oscillators", *J. Opt. Soc. Am. B* **18**, pp. 1732-1741, 2001.
17. M. Sheik-Bahae, D.C. Hutchings, D.J. Hagan, E.W. van Stryland. "Dispersion of bound electronic nonlinear refraction in solids", *IEEE J. Quantum Electron.* **27**, pp. 1296–1309, 1991.
18. V.L. Kalashnikov, E. Sorokin, I.T. Sorokina. "Multipulse operation and limits of the Kerr-lens mode locking stability", *IEEE J. Quantum Electron.* N2, 2003 (in press).
19. N.N. Akhmediev, V.V. Afanasjev, J.M. Soto-Crespo. "Singularities and special solutions of the cubic-quintic complex Ginzburg-Landau equation," *Phys. Rev. E*, **53**, pp. 1190–1201, 1996.
20. detailed investigations show some interesting modification of the single pulse stability and its spectral characteristics, see V.L. Kalashnikov, S. Naumov, E. Sorokin, I. Sorokina, "Spectral broadening and shift of the few optical cycle pulses in  $\text{Cr}^{4+}:\text{YAG}$  laser," in Program of ASSP'2003, San Antonio, USA, February 2-5, TuB1, 2003.